ELSEVIER

Journal of Materials Processing Technology 102 (2000) 257–265

Journal of Materials Processing Technology

www.elsevier.com/locate/jmatprotec

Finite element modeling of sheet-metal blanking operations with experimental verification

Ridha Hambli[a,*], Alain Potiron[b,1]

[a]ISTIA — LASQUO, 62, Avenue Notre dame du Lac, 49000 Angers, France
[b]ENSAM — LPMI, 2, Boulevard du Ronceray, B.P 3525, 49035 Angers cedex, France

Accepted 25 January 2000

Abstract

In order to accurately simulate sheet-metal cutting processes by material shearing mechanisms, such as blanking and punching processes, a finite element model valid for the numerical description of such processes has been developed. Damage and crack propagation have been taken into account by means of an elastoplastic constitutive law. To study the effects of variation of processes parameters on the geometry of sheared edges and the force-punch penetration evolution, we have implemented the algorithm of calculation by means of users routine (UMAT) of ABAQUS/Standard finite element code. Final results of the FEM simulation agree with the experimental ones. © 2000 Published by Elsevier Science S.A. All rights reserved.

Keywords: Von Mises yield criterion; Finite element modeling; Material shearing mechanisms

Nomenclature

$\boldsymbol{B}$	strain–displacement matrix
C_c	critical value of a failure criteria
D	damage variable
D_c	critical damage value at fracture
D_R	damage value at which the damaged finite elements break
$\mathbf{E}$	Hooke elastic operator
f	yield function coupled with damage
$\boldsymbol{J}_n^r$	Jacobien tensor at increment (n) and iteration (r)
$\boldsymbol{K}_n^r$	stiffness matrix at increment (n) and iteration (r)
U_n	displacement field at increment (n)
σ_{el}	initial yield stress
σ_0	isotropic non-linear hardening law
σ_{eq}	equivalent Von Mises stress
σ_H	hydrostatic pressure
σ_{ij}	stress tensor components
σ_n^T	elastic prediction of the stress tensor components at increment (n)
σ_n	stress tensor at increment (n).
σ_{n+1}	Cauchy stress tensor at increment ($n+1$)
ε_{eq}	equivalent plastic strain
ε_D	threshold logarithmic strain at which Le Maître damage initiates
ε_R	logarithmic strain value at fracture
ε_{tot}	total strain tensor
ε_{ij}	strain tensor components
ε_{el}	elastic part of te strain tensor
ε_{pl}	plastic part of te strain tensor
$\Delta\varepsilon$	strain increment
λ	plastic multiplier
λ_e, μ_e	Lamé constants

1. Introduction

Sheet-metal working by material shearing mechanisms is one of the most frequently used processes in industry. Depending on the position of the sheared surface with respect to the workpiece coordinates, various shearing processes are used, such as blanking, piercing and cutting off [16]. Contrary to other operations, such as stamping and folding where the aim is to plastically deform the sheet, blanking operations lead to the total rupture of the sheet.

* Corresponding author. Tel.: +33-2-41-36-57-57.
E-mail addresses: ridha.hambli@istia.univ-angers.fr (R. Hambli), alain.potiron@univ-angers.fr (A. Potiron)
[1] Tel.: +33-2-41-20-73-73.

PII: S0924-0136(00)00496-9

As the process is performing, the material whose behavior is non-linear, is subjected to complex strain and stress states [4,11]. Before complete rupture, the material is subjected to some phenomena of damage and crack propagation. To describe the sheet's behavior as the operation is carried out, various parameters may be used such as the material state of hardening and damage.

From a numerical point of view, a good description of the whole process requires the development of reliable algorithms. These allow the crack initiation and propagation phenomena to be modeled accurately and without computational divergence. In previous studies [8,12,20,21], that have dealt with this topic, simplified hypotheses were used, sometimes in a rather coarse manner.

The aim of this paper is to provide a general FEM allowing for the numerical simulation of the whole blanking process. The numerical results obtained by the simulation were compared with experimental ones to verify the validity of the FEM proposed.

2. Sheet-metal shearing simulation

Numerous works have developed elaborate numerical models, using FEM to simulate sheet-metal shearing processes. Popat et al. [21] in 1989, used an FE modeling allowing for the simulation of a blanking operation from the beginning of the process until the initiation of macro-cracks. The material of the sheet is assumed to be isotropic, linearly elastic, linearly strain hardening and to follow the Von Mises yield criterion. A fracture criterion of equivalent-strain type was introduced to include the initiating step of the cracks. The authors postulated that a crack is initiated at any point in the sheet when the effective strain reaches the fracture strain value of the material. The program is stopped using the aforementioned criterion, when the cracks are initiated at any point of the sheet. From this study, it can be observed that

- to simulate the contact between the punch, the die and the sheet, the authors have applied boundary conditions that are considered stable as calculation is carried out, neglecting the bending of the sheet,
- the damage phenomenon was not accounted for and the final rupture was not simulated.

Hartley et al. [13] improved the previous model by taking into account the management of contact between the tool and the sheet. Various criteria for predicting the fracture of the material during the operation were adopted by the authors. As in previous works, it can be noted that the progressive damage of the sheet's material was not included into the formulation of constitutive laws and the program used for analysis was not suitable for simulating the propagation of the fracture across the sheet.

Maillard [20] attempted to simulate the blanking operation with the help of the FE code CASTOR-EVP2D, until the penetration of the punch reaches 40% of the sheet's thickness. The material of the sheet was assumed to be isotropic, linearly elastic and non-linearly strain hardening. Stages of initiation and propagation of cracks were modeled by using two ductile rupture criteria, the first of which being similar to that of Rice and Tracey [22] and the second one being based upon an equivalent plastic deformation. When the chosen criterion reaches its critical value, the author abruptly sets the stiffness of the element to zero. It may be noted again that the continuously damaging of the material was not accounted for and that the final rupture could not be simulated. Recently, Homsi et al. [12] applied the Gurson model [9] which accounts for the material damage, in order to describe the behavior of the sheet. In this approach, the damage variable f_v is defined as the volume fraction of the voids in the material. In this way, the authors were able to simulate the blanking operation up to a punch penetration to the order of 45% of the sheet's thickness. Nevertheless, the final rupture was not simulated.

3. Behavior of the sheet

The law describing the material behavior should allow for the description of the different stages of the process observed experimentally starting from the elastic state and ending in the final rupture of the sheet. For this, a behavioral law including damage and failure phenomena must be chosen. The development of a simulation for sheet-metal shearing operations may be carried out according to the schematic diagram given in Fig. 1.

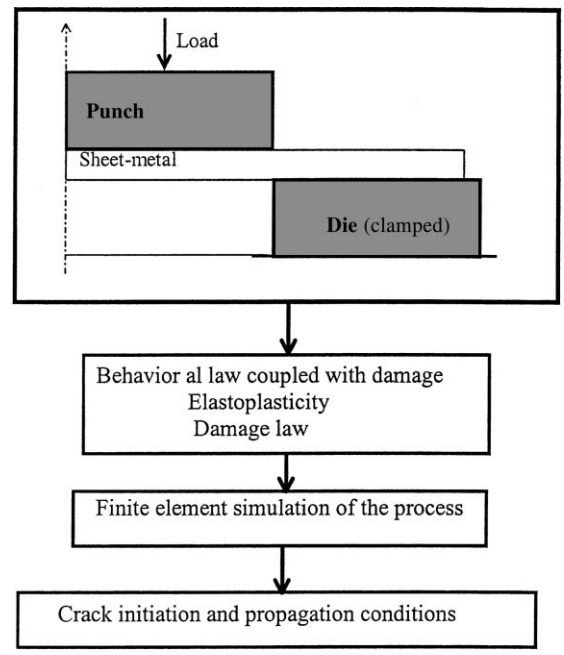

Fig. 1. Schematic diagram of the approach used.

3.1. Numerical modeling of damage and ductile fracture

Inspection of the most recent studies in the field of industrial process simulation shows that, despite the increasing progress in numerical computational methods, there is still a lack of models dealing with sheet-metal shearing processes which include ductile damage and fracture phenomena.

Recently, Clift et al. [5] carried out a comparative study by means of FEMs, which included failure of the material, in order to investigate metal forming problems. The failure was numerically predicted by means of several criteria. Comparing the numerical and the experimental results they concluded that some criteria which are well suited to simulate the behavior of the material for certain particular processes and geometries, cannot be used efficiently in other cases. There is not an universal failure criterion which allows for the description of any industrial metal forming process.

3.1.1. Ductile fracture criteria

In order to predict when a structure will undergo rupture, numerous authors have proposed their own criteria. In the isotropic case, these failure criteria are scalar functions involving stresses and/or strains, which depend on physical and mechanical parameters. They are usually identified by performing rheological tests on specimens. The failure is modeled by a mathematical function which is supposed to represent the physical behavior of the material, and occurs when the function reaches a critical value C_c. The functions are often written in the following form:

$$\text{If} \quad \int_0^{\varepsilon_R} f(\sigma, \varepsilon_{eq})\, d\varepsilon_{eq} - C_c < 0 \quad \text{there is no failure.} \tag{1}$$

$$\text{If} \quad \int_0^{\varepsilon_R} f(\sigma, \varepsilon_{eq})\, d\varepsilon_{eq} - C_c \geq 0 \quad \text{the failure occurs.} \tag{2}$$

In the above expressions, ε_R is the strain at rupture, ε_{eq} the equivalent plastic strain defined by means of the plastic part

$$\varepsilon_{eq} = \sqrt{\tfrac{2}{3}\varepsilon_{ij}^{pl}\varepsilon_{ij}^{pl}} \tag{3}$$

Different failure criteria which can be applied to predict the ultimate elastoplastic behavior of structures subjected to external forces have been detailed by Hambli Ridha [11]. It can be shown that these criteria are not suitable for describing the gradual material-degradation which cause the first crack initiation. Consequently, theoretical formulations have been developed by means of elastoplastic laws coupled with continuous damage. In the following, we refer to the work of Le Maître and Chaboche [17].

In this, the isotropic damage variable D is defined by the ratio between the total area S_D of the micro-cracks and cavities and the overall sectional area S as follows:

$$D = \frac{S_D}{S} \tag{4}$$

The concept of effective stress associated with the previous definition suggests that the damage affects the elasticity modulus E and the yield criterion. The experimental damage law is determined by a tension test [7,14,18].

4. Finite element study

The algorithms generally implemented in the FE codes for the integration of the constitutive equations in an incremental form are the so-called radial return algorithms. They are based upon the notion of an elastic-predictor–plastic-corrector where a purely elastic trial-state is followed by a plastic-corrector phase [1,3].

The Newton method is used to solve the non-linear global equilibrium equations as well as the non-linear local equations obtained by full implicit integration of the constitutive equations.

The consistent local tangent modulus is obtained by exact linearization of the algorithm. In comparison with the use of the analytical 'standard' modulus, the consistent modulus leads to a faster convergence rate when the Newton algorithm is used to perform iterations in the balance equations. In this way, an implicit algorithm has been developed which allows for the integration of the constitutive equations. The scheme retained seems well suited to handle the non-linearity of the behavioral law [10,19].

The procedure described, was implemented in the general purpose code ABAQUS/Standard with the help of the user subroutine UMAT [1,2].

4.1. Global equilibrium equations

Within the framework of the displacement formulation of FEM, the global equilibrium equations to be satisfied at each instant t_{n+1} can be written in the general form [1]

$$\boldsymbol{F}(U_{n+1}) = 0 \tag{5}$$

U_{n+1} is the displacement field at increment $(n+1)$.

If this non-linear problem is solved iteratively by a Newton method, at each global iteration r the following equation can be written:

$$\boldsymbol{F}(U_{n+1}^r) + \boldsymbol{K}_{n+1}^r(U_{n+1}^{r+1} - U_{n+1}^r) = 0 \quad \text{with} \quad U_{n+1}^0 = U_n \tag{6}$$

where

$$\boldsymbol{K}_{n+1}^r = \left(\frac{\partial \boldsymbol{F}}{\partial U}\right)_{n+1}^r = \int_\Omega \boldsymbol{B}^T \boldsymbol{J}_{n+1}^r \boldsymbol{B}\, d\Omega\, d\Omega \tag{7}$$

where $\boldsymbol{B}$ is the strain–displacement matrix and $\boldsymbol{J}_{n+1}^r$ an approximation of $(\partial\sigma/\partial\varepsilon)_{n+1}^r$

4.2. Local integration

From a numerical point of view the problem consists in resolving the constitutive equations describing the behavior of the sheet.

The set of equations defining the problems are derived from the following:

1. The decomposition of the deformation into an elastic part and a plastic part:

$$\varepsilon_{\text{tot}} = \varepsilon_{\text{el}} + \varepsilon_{\text{pl}} \tag{8}$$

2. The elastic law coupled with Le Maître damage law:

$$\sigma_{ij} = (1 - D)(\lambda_{\text{e}}\delta_{ij}\varepsilon_{kk}^{\text{el}} + 2\mu_{\text{e}}\varepsilon_{ij}^{\text{el}}) \tag{9}$$

or in Jaumann (corotational) rate form:

$$\dot{\sigma}_{ij}^{\text{J}} = (1 - D)(\lambda_{\text{e}}\delta_{ij}\dot{\varepsilon}_{kk}^{\text{el}} + 2\mu_{\text{e}}\dot{\varepsilon}_{ij}^{\text{el}}) \tag{10}$$

where λ_{e} and μ_{e} are Lame's constants.

3. The plastic flow law (implicit scheme):

$$\Delta\varepsilon_{\text{pl}} = \Delta\lambda\frac{\partial f}{\partial\sigma}, \quad \lambda \text{ being the plastic multiplier.} \tag{11}$$

4. The integration of the damage law:

$$D = D(\sigma_{ij}, \varepsilon_{ij}, a_k) \tag{12}$$

where a_k indicates the intrinsic coefficients of the material.

5. The integration of the yield function coupled with damage:

$$f = \sigma_{\text{eq}} - (1 - D)(\sigma_{\text{el}} + \sigma_0) \tag{13}$$

σ_{el} is the initial yield stress, and σ_0 the isotropic non-linear hardening law.

The integration methods of the non-linear constitutive equations are based on the use of a special algorithm which solves the equations in incremental form. For this purpose, during a small time interval $[t_n, t_{n+1}]$, it is supposed that the whole increment is purely elastic, then an elastic prediction is defined as follows:

(a) *Elastic-predictor.*

$$\sigma_{n+1}^{\text{T}} = \sigma_n + \Delta\sigma = (1 - D_{n+1})\mathbf{E}\varepsilon_{\text{tot}} \tag{14}$$

E is the Hooke elastic operator. If this elastic-predictor satisfies the yield condition, $f<0$ the prediction is true and the local procedure is completed. Then it can be stated that:

$$\sigma_{n+1} = \sigma_{n+1}^{\text{T}} \tag{15}$$

Otherwise, this state must be corrected by means of a plastic correction defined by the following development:

Plastic correction. The variables at t_{n+1} must satisfy the yield condition, i.e. the evolution laws written in the incremental form and elasticity law must satisfy the system:

$$f = 0 \tag{16}$$

$$\sigma_{n+1} - (1 - D_{n+1})\mathbf{E}(\varepsilon_n + \Delta\varepsilon - \varepsilon_n^{\text{pl}} - \Delta\varepsilon^{\text{pl}}) = 0 \tag{17}$$

In this case, we must project the stresses σ_{n+1}^{T} on the surface of the yield function δf, as follows:

$$\sigma_{n+1} = P\left(\sigma_{n+1}^{\text{T}}\right) \tag{18}$$

where $P : R^5 \rightarrow \delta f$ denotes the orthogonal projection on δf of the trial stresses σ_{n+1}^{T}.

4.3. Choice of the damage model

The metal cutting operation depends on the damage caused to the material. The accurate knowledge of the material failure process is an essential stage in the selection of a damage model. In the case of sheet blanking by shearing processes, numerous authors have studied the different physical mechanisms leading to the final rupture and proposed their own models.

Dos Santos and Organ [6] carried out a viscoplastic study of a rectangular-bar cropping operation. They analyzed the deformation of a pattern engraved on the surface of the sheared area of the testing bar. They demonstrated, by means of this observation that the rupture is of a ductile nature and that the cracks generated by the cropping process follow an 'S', or double 'S' profile, parallel to the maximum intensity of the shear stress.

Examining the facies of the sheared edge, Jana and Ong [14], confirmed that the blanked edge exhibits microscopic hemispherical holes which characterize the ductile fracture.

Starting from a different approach which states that the moment when cracks initiate, the hydrostatic pressure σ_{H} is negative at the cutting edges of the tools, Kasuga et al. [15] proposed a theoretical model for the damage propagation. They showed that the cracks which begin at the cutting edges of the die and the punch grow and spread in the direction of the material where σ_{H} is minimum. Finally, Hambli Ridha [11] while describing the fundamental fracture mode which occurs in metal sheet blanking, determined that it is the equivalent plastic strain which is the main parameter. When it exceeds a critical value, the fracture of the material takes place. As a conclusion from the aforementioned works, it is obvious that a damage law must take into account the equivalent plastic strain and the hydrostatic pressure value σ_{H}. Such a law would be suitable to describe the damage process of the material before final rupture.

In the model of isotropic damage evolution of Le Maître [17] the damage law is written in the incremental form:

$$\text{d}D = \frac{D_{\text{c}}}{\varepsilon_{\text{R}} - \varepsilon_{\text{D}}}\langle Rv\text{d}\varepsilon_{\text{eq}} - \varepsilon_{\text{D}}\rangle \tag{19}$$

σ_{H} is included in the Rv term:

$$Rv = \frac{2}{3}(1 + \nu) + 3(1 - 2\nu)\left(\frac{\sigma_{\text{H}}}{\sigma_{\text{eq}}}\right)^2 \tag{20}$$

ν is the Poisson coefficient, ε_{D} the threshold logarithmic strain at which damage initiates, ε_{R} the logarithmic strain value at fracture and ε_{eq} the logarithmic plastic strain. D_{c} is the critical damage value at fracture. The operator $\langle\ \rangle$ means that $\langle X\rangle = X$ if $X>0$ and $\langle X\rangle = 0$ if $X\leq 0$.

This model requires the knowledge of the three parameters D_{c}, ε_R and ε_D which are easily identified by means of a tensile test [11,14].

4.4. Cracks initiation and propagation simulation

During the analysis, the initiation of crack is supposed to occur at any point in the structure where the damage reaches its critical value D_c. The crack propagation is simulated by the propagation of a completely damaged area. This is taken into account in the FEM by a decrease in the stiffness of the elements concerned.

4.5. Interface modeling

Modeling the interaction between the tool and the sheet is one of the most important considerations necessary to simulate the blanking process correctly. Modeling the contact at the interfaces between the sheet and the tool, is handled by adopting a rigid body hypothesis and contact surface laws defined by a Coulomb friction model with a friction coefficient value of 0.15.

5. Numerical simulation of a blanking operation

The problem studied here consists of an axisymmetric blanking operation of a sheet-metal with 3 mm thickness. The geometrical data is shown in Fig. 2.

The mechanical characteristics of the material obtained by a tensile test are:

$E = 210\,000\,\text{MPa}, \quad v = 0.29$

The corresponding strain hardening law takes the non-linear form (Fig. 3):

$$\sigma = \sigma_{el} + K\varepsilon_{pl}^{n} \tag{21}$$

with the values of σ_{el}=250 MPa, K=1048 MPa and n=0.196.

The rheological constants for the damage law associated with the Le Maître model were found to be: ε_D=0, ε_R=0.8 and D_c=0.37.

5.1. Selection of the mesh

In this particular FEM simulation, the selection of the mesh is of great importance because it must be suitable

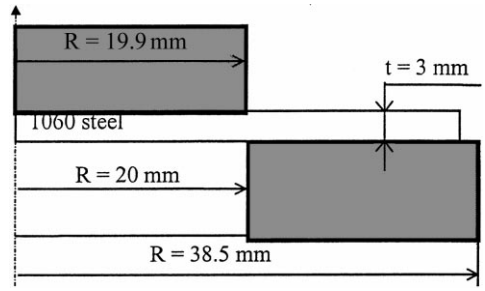

Fig. 2. Axisymmetric model of the blanking operation.

to describe the phenomenon of crack initiation and propagation. Therefore refining the mesh in the clearance between the punch and the die is essential throughout the thickness of the sheet. Inside the regions where the material is not subjected to high stress levels, a coarse mesh is sufficient.

The meshing of the model is carried out by means of 1400 quadrangular four node axisymmetric elements. Fig. 4 shows how the mesh has been constructed.

6. Results and discussion

Experiments using devices equipped with electrical gauges and force tranducer were performed by a 4000 kN hydraulic press in order to verify the validity of the proposed FEM.

For the first time, a simplified simulation of the blanking process was performed neglecting damage. Using the aforementioned algorithm in which the damage value is set to zero, it is possible to simulate the punch penetration up to 100% of the sheet's thickness, in spite of a large mesh distortion. The corresponding results are now to be compared to those deduced from the whole theory including damage.

When the material damage is taken into account, the same punch penetration has been reached, but with a computing time about 1.7 times greater. This increase in computing time is caused by the numerical convergence which is more and more difficult to obtain, as the damage reaches the

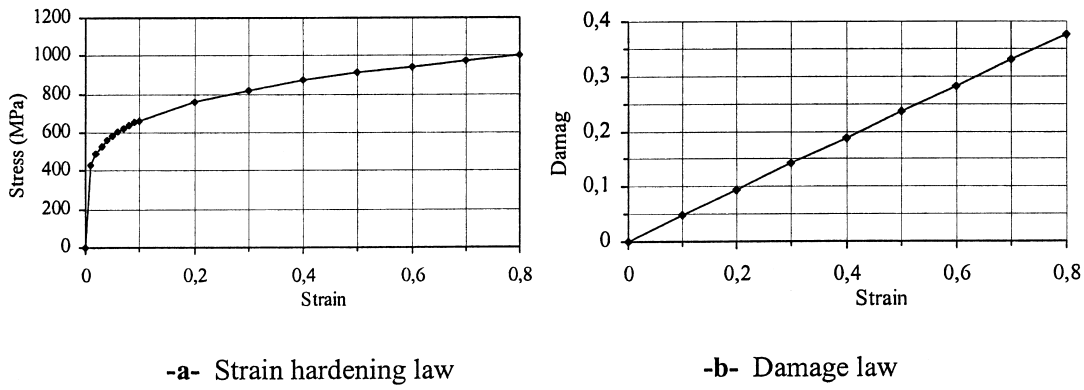

-a- Strain hardening law -b- Damage law

Fig. 3. Strain hardening and damage law for 1060 steel (experimental data).

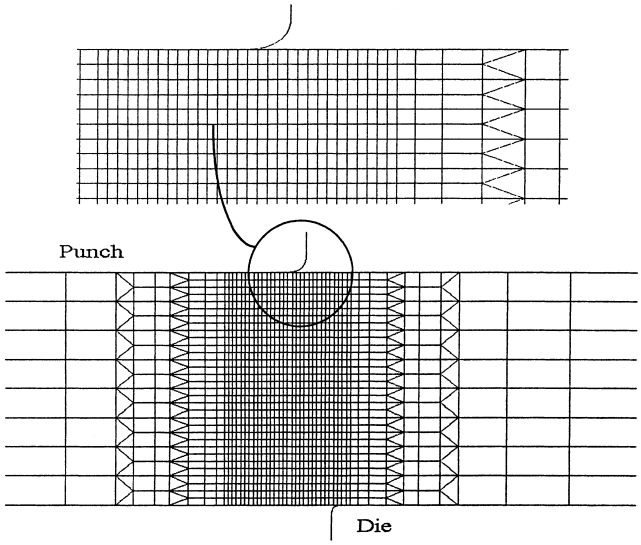

Fig. 4. Mesh used for the FE model.

critical value D_R at which the damaged finite elements will break.

As the optimal choice of the press and corresponding tools is always an industrial goal, the punch force vs. the punch displacement during the blanking process has been computed. In Fig. 5, in the case of an optimal relative clearance of 10% of the sheet thickness, three curves are drawn. These correspond to the numerical predictions, and the experimental results.

It can be seen that the more realistic description of the process corresponds to the model that includes damage. Consequently it can be concluded that to be accurately predicted, the blanking process would necessarily account for damage. The failure of the sheet presented in Fig. 6 is obtained for a punch displacement of about 70% of the sheet thickness. Data for the numerical modeling correspond to those of the sheet used in experiments.

The computation results corresponding to different displacement steps of the punch penetration and the corresponding graphical issues are presented in Fig. 7. The crack propagation in the mesh up to final rupture can be observed.

Referring to Figs. 6 and 7d show that the predicted blanked profile is in good agreement with the experimental one.

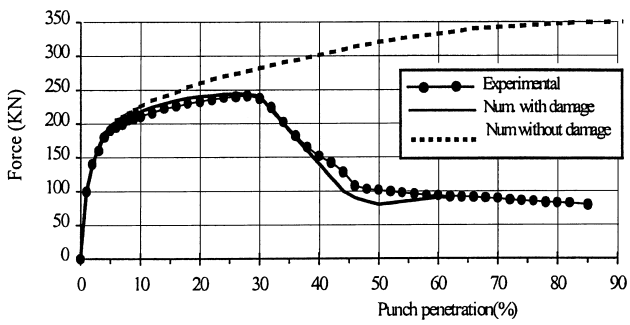

Fig. 5. Punching forces against punch travel.

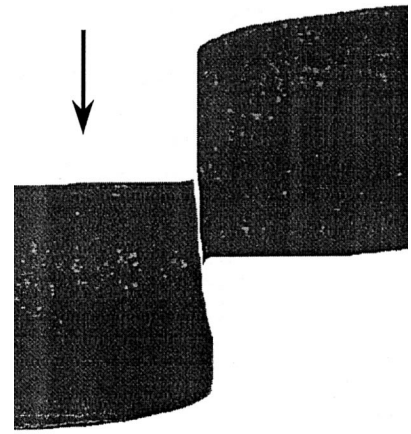

Fig. 6. Experimental blanked profile (relative clearance=10%).

As it can be observed, the distortion of the mesh is restricted to a small area near the die–punch clearance.

Despite all non-linearities arising from contacts between the sheet and the tools and elastoplastic behavior of the material, the results demonstrate the robustness and reliability of the algorithm.

6.1. Influence of the tool wear

The design of the tool is one of the main features in the industrial process. Therefore it is necessary to compute, as accurately as possible, all the forces acting on the sheet and the tool. For this purpose, several calculations were performed in order to compare the numerical results with experimental data. The influence of the tool wear on the punching force and on the evolution of the sheared profiles was accounted for by changing the values of the edge radii Rp and Rd (Fig. 8).

Four geometric shapes of the tool were chosen corresponding to:

- a new die with Rd=0.01 mm,
- a new punch with Rp=0.01 mm,
- three punches with different edge radii Rp=0.06, 0.12 and 0.2 mm.

The comparison between the results obtained by the FE and those obtained by experiment can be seen in Fig. 9a and b.

In Fig. 9a, the evolution of the punching forces relative to the punch penetration for different simulations are shown.

The experimental plots on Fig. 9b shows that for the various states of punch wear, there is no difference between the maximum blanking loads. Neverthless, the punch penetration corresponding to the crack initiation in the sheet-material increases with an increase in punch wear. This is due to relative increase in the contact area between the punch and the sheet.

From a competitive industrial point of view, the best quality of mechanical parts must be obtained with minimum

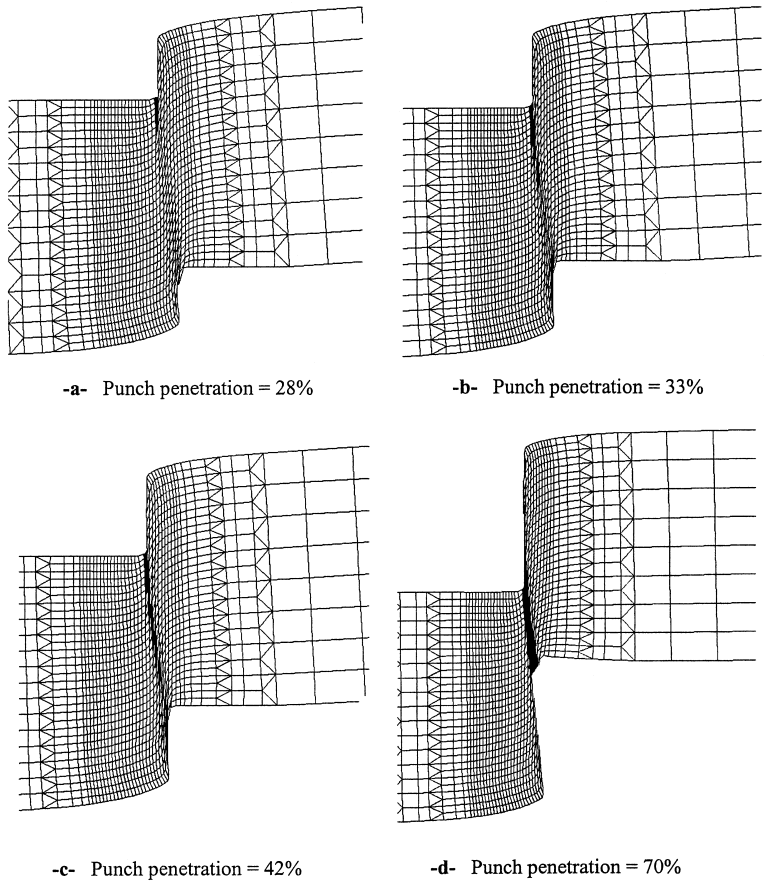

Fig. 7. Crack propagation in the mesh (relative clearance=10%).

costs. Therefore attention was also focused here on the geometrical quality of the blanked profile.

Two blanked profiles corresponding to a new punch with a cutting edge radius Rp=0.01 mm and a used punch with Rp=0.2 mm are shown in Fig. 10a and b. It was verified in [8] that the numerical prediction was in very good agreement with the experimental results.

As it can be expected, in the case of a used punch, the profile of the part boundary presents a bad quality due to the presence of a burr.

The numerical results compared with the experimental ones, show the reliability of the FEM according to the aforementioned damage laws in describing the influence

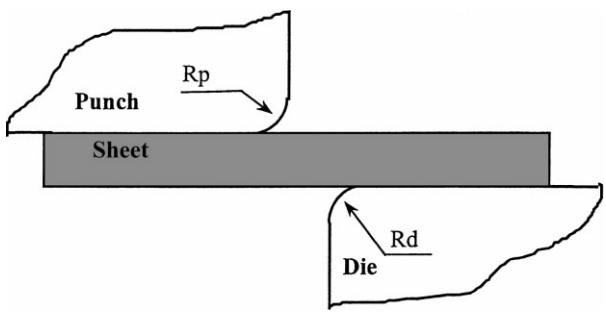

Fig. 8. Geometry of the cutting edges of the tool.

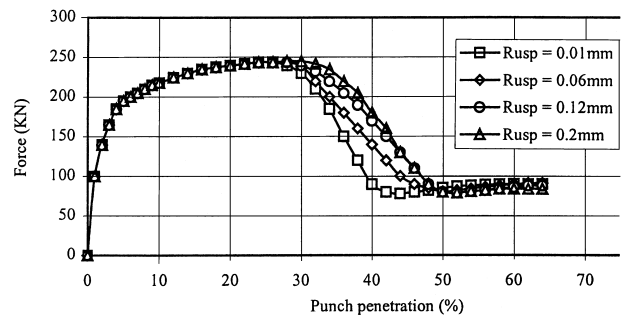

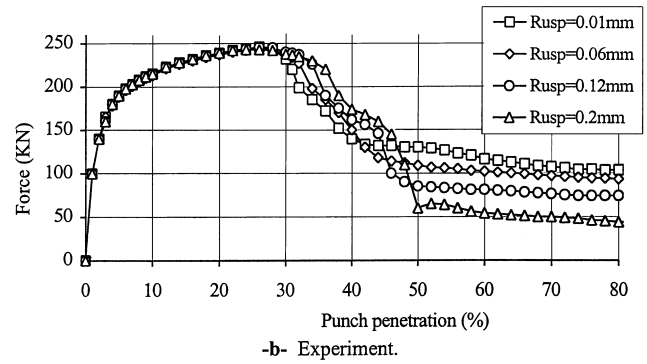

Fig. 9. Punching force vs. punch travel for four wear states.

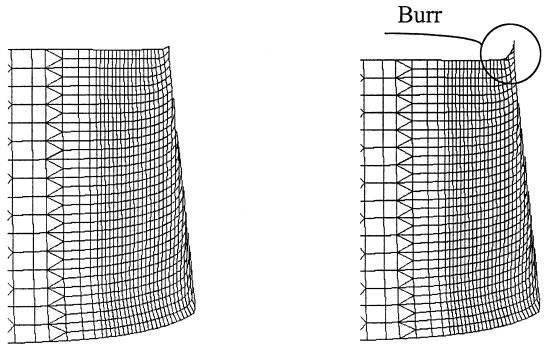

-a- New punch : Rp = 0.01 mm. -b- Used punch Rp = 0.2 mm.

Fig. 10. Predicted profiles corresponding to two states of the punch wear (clearance=10%).

of punch wear on the mechanical results in the case of blanking operation processes.

6.2. Metal flow prediction

The material flow caused by the penetration of the punch into the sheet was carefully investigated by blanking circular test specimens with concentric circular tools.

The experiment was performed to confirm that the FE model was sufficiently accurate in the prediction of all mechanical effects of a blanking operation.

In order to detect the orthoradial strains of the specimens during the blanking operation, five strain gauges were bonded on the upper surface of the specimens at radial distances varying from 2 to 10 mm from the cutting edge of the punch. A schematic illustration of the experimental apparatus is shown in Fig. 11.

The evolutions of the orthoradial strains vs. punch penetration during the blanking operation, as recorded by the five gauges, are plotted in Fig. 12b. The corresponding five curves obtained by the FE simulation are drawn in Fig. 12a.

It can be observed that, the closer the gauge to the sheared of the sheet, the higher the amplitude of the strain.

The obvious agreement between the numerical results and the experimental data confirms the reliability of the FEM algorithm in describing the flow of the sheet material during the process.

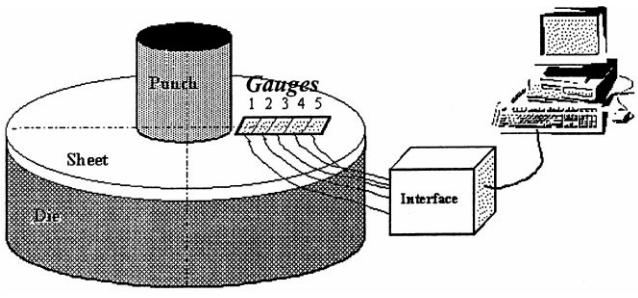

Fig. 11. Schematic illustration of the testing device.

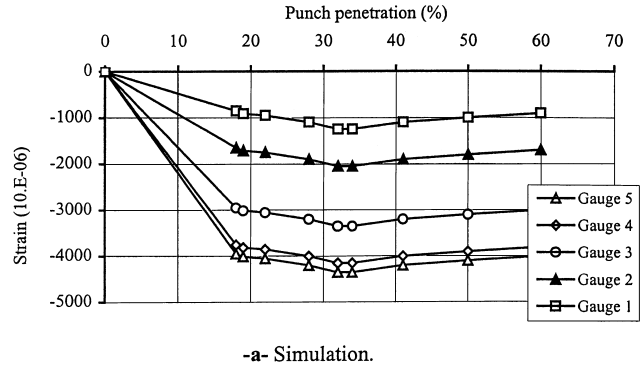

-a- Simulation.

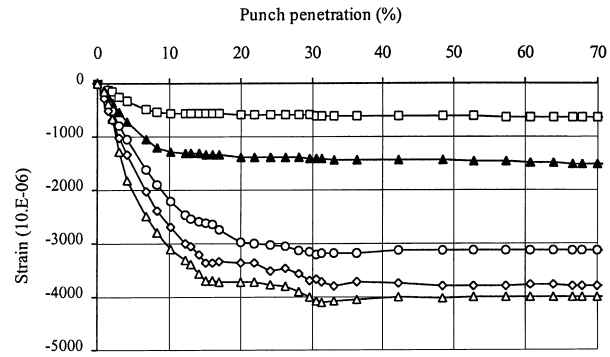

-b- Experiment.

Fig. 12. Orthoradial strains vs. punch penetration.

7. Conclusion

Sheet-metal blanking is one of the main industrial process for forming mechanical parts, therefore attention must be focused on its simulation. It has been shown that an accurate simulation of the process leads to an optimal choice of forming parameter.

The material behavior has to be accurately known, especially in accounting for damage evolution and rupture simulation. A realistic and sufficient damage law is the Le Maître and Chaboche's one which leads to good predictions in the simulation of blanking processes. It was noted that the choice of large displacements formulation, an incremental algorithmic process, and complex behavioral law do not have any influence on the numerical convergence of the computational scheme.

The crack initiation and propagation can be predicted accurately without computational divergence from the moment of crack initiation to the complete rupture of the sheet-part. throughout the process simulation, experimental and numerical results are always in good agreement.

From a computational point of view, the results obtained by means of ABAQUS/Standard routines, which account for the contact law between tool and sheet and incremental computations strategy, give good results compared to experimental ones. For relative punch penetrations up to 70%, the distortion of the FE are still satisfactory and calculations can be done without problems.

From a practical point of view, simulation can provide useful information about the influence of the tool-wear on the quality of the external shape of the blanked parts.

Acknowledgements

The authors would thank Devillé S.A Industry for its support.

References

[1] ABAQUS–HKS Theory Manual, Version 5.4.
[2] ABAQUS User's Conference, Writing a (V) Umat, Aachen, Germany, June 1993.
[3] M.A. Criesfield, Non Linear Finite Element Analysis of Solids and Structures, Vol. 1, Wiley, New York, 1991.
[4] M. Cervenka, B. Bouchet, C. Gasc, Influence du mode de découpage sur le comportement en fatigue de tôles minces d'aciers dual-phase, Mém. Sci. Rev. Métall., 1990, pp. 185–194.
[5] S.E. Clift, P. Hartley, C.E.N. Sturgess, G.W. Rowe, Fracture prediction in plastic deformation process, Int. J. Mech. Sci. 32 (1) (1990) 1–17.
[6] W. Dos Santos, A.J. Organ, Deformation in the ductile fracture processes examined by the viscoplasticity method, Int. J. Mach. Tool. Des. Res. 13 (1973) 102–112.
[7] J. Dufailly, Modélisation mécanique et identification de l'endommagement plastique des métaux, Thése de Docteur de 3éme cycle, Univ. Pierre et Marie Curie, Paris, Vol. 6, 1980.
[8] M.M. El Menni, Dubois, M. Gelin, Traitement de problémes numériques liés à la modélisation par éléments finis du processus de découpages des métaux, Strucome 93 (1993) 568–578.
[9] A.L. Gurson, Continium theory of ductile rupture by void nucleation and growth, J. Eng. Mater. Technol. Trans. ASME 99 (1977) 2–15.
[10] J.C. Gelin, Modéles numériques et expérimentaux en grandes déformations plastiques endommagement de rupture ductile, Thése de Doctorat d'Etat, Paris, Vol. 6, 1985.
[11] H. Ridha, Etude expérimentale, numérique et théorique du découpage des tôles en vue de l'optimisation du procédé (in French), Thése de Doctorat ENSAM d'Angers, October 15, 1996.
[12] M. Homsi, M. Wronski, J.M. Roelandt, Modélisation numérique de la coupe, Strucome 94 (1994) 677–690.
[13] P. Hartley, I. Pillinger, C. Sturgess, Numerical Modeling of Material Deformation Processes Research, Development and Applications, Springer, Berlin, 1992.
[14] S. Jana, N.S. Ong, Effect of punch clearance in the high-speed blanking of the thick metal using an accelerator for mechanical press, J. Mech. Work. Technol. 19 (1989) 55–72.
[15] Y. Kasuga, S. Tsutsumi, T. Mori, Investigation into shearing process of ductile sheet metals, Mem. Fac. Eng. Nagoya Univ., Japan, 1979, pp. 1–46.
[16] K. Lange, Handbook of Metal Forming, McGraw-Hill, New York, 1985.
[17] J. Le Maître, J.L. Chaboche, Mécanique des Matériaux Solides, 2ème édition, Dunod, Paris, 1988.
[18] F. Montheillet, F. Moussy, Physique et Mécanique de l'endommagent, Les éditions de Physique, 1986.
[19] J.M.M.C. Marques, Stress computation in elastoplasticity, Eng. Comput. 1 (1984) p. 42–51.
[20] A. Maillard, Etude expérimentale et théorique du découpage, Thése de doctorat Université de Technologie de Compiégne, 1991.
[21] P.B. Popat, A. Ghosh, N.N. Kishore, Finite element analysis of the blanking process, J. Mech. Work. Technol. 19 (1989) 269–282.
[22] J.R. Rice, D.M. Tracey, On the ductile enlargement of voids on triaxial stress fields, J. Mech. Phys. Solids 17 (1969) 201–217.